J. Membrane Biol. 24, 201 – 223 (1975)

Ionic Dependence of Sodium Currents in Squid Axons Analyzed in Terms of Specific Ion "Channel" Interactions

M. Cohen, Y. Palti and W.J. Adelman, Jr.

Dept. of Physiology and Biophysics, Technion School of Medicine, P.O.B. 9649, Haifa, Israel, Laboratory of Biophysics, NINDS, NIH, Bethesda Md. 20014, and The Marine Biological Laboratory, Woods Hole, Mass. 02543

Received 5 September 1974; revised 5 June 1975

Summary. Inward sodium currents were measured from voltage-clamped giant axons externally perfused with artificial seawater (ASW) solutions containing various concentrations of sodium and potassium ions. The data was analyzed under the assumption that under a constant membrane potential sodium conductance is determined by a specific ion-channel site (SIS) reaction. The sodium current density values were expressed in terms of SIS-reaction rates which were compared, by means of minimization techniques, with those computed for various saturation reaction mechanisms. The following conclusions were drawn:

1) The dependence of peak inward sodium current on external sodium and potassium concentrations can be described in terms of saturation reactions.

2) The experimental data fit well the kinetics of a positive cooperative homotropic reaction, involving at least two allosteric active sites. One of these sites may be catalytic while the other, either catalytic or regulatory.

3) The inhibitory effect of external potassium on inward sodium current, can be described by a reversible competitive or noncompetitive inhibition mechanism. The values of the dissociation constant of the inhibitor-site "complex" (K_i) were found to be close to the external potassium concentration under physiological conditions.

The ionic currents associated with nerve excitability are driven by electrochemical potential gradients and controlled by a voltage-dependent gating mechanism (Hodgkin & Huxley, 1952). One of the basic assumptions of the Hodgkin-Huxley model, which describes such axon behavior, is that in the "pathway" beyond the gate the ionic flow can be described, to a good approximation, by electro-diffusion processes (the independence principle). In such processes the ionic currents are linearly related to the ion concentration. However, more recent data indicate that the above may not be true. For example, inward potassium current was shown (Hodgkin & Keynes, 1955*b*) to be nonlinearly related to external potassium concentration (at a constant membrane potential), external potassium

was found to inhibit inward sodium current (Adelman & Palti, 1969*a*, *b*), and this effect was found to be voltage-dependent. Furthermore, Hille (1972, 1975) has recently described experiments dealing with the dependence of inward sodium currents on external sodium or sodium substitutes' concentration. These experiments which contradict the independence principle, also suggest competition at the sodium site.

The above findings are consistent with models which propose that at some stage, the ion passage is mediated by a specific ion-site[1] interaction (Adelman & Palti, 1969*b*; Fishman, Cherneikin & Volkenstein, 1973).

Such a specific ion site (SIS) reaction, which facilitates ion passage through the membrane[2], involves interaction with a very limited number of active sites which are assumed to remain intact at the end of the process. Therefore, within this framework the "ionic channel" mechanism may be treated using enzyme kinetics methods.

An ion-site interaction in the channel can take place at the "gate" or "pathway" level. If we assume that the ionic interaction at the "gate" results in modification of the "gate" characteristics, it is to be expected that it will affect the time and or voltage dependency of the conductance (change m, n, h and the τ's). In contrast, an interaction on the pathway level can be expected to result in a so-called $\bar{g}$ effect, i.e. its effect should be independent of voltage and time.[3]

Since variations in Na^+ and K^+ concentrations were shown to affect membrane conductance, including its voltage and time dependency, one may conclude that the major effect of the ion-site interaction is on the gate level.

It is the purpose of this work to investigate the possibility that membrane sodium current is determined at least in part, by specific ion-site (SIS) interactions. Within this framework the dependence of sodium current on external sodium and potassium concentrations will be analyzed and an attempt will be made to determine the type of reaction which fits the data best. To avoid the additional complexity, which may result from the voltage dependency of the ionic effect, all parameters will be determined at a constant membrane potential (zero mV).

---

1 A site here would be any membrane channel element with which the ion involved in the permeation process interacts (*see also* Appendix I, Part 1).

2 Under physiological conditions the penetrating ions do not possess the energy required to pass through the lipid membrane (Ehrenstein & Lecar, 1972).

3 It is possible, although not very probable, that an ion-pathway interaction would modify the pathway such as to become time and voltage dependent. Such an effect would be manifested in a superposition of a new voltage and time dependency on top of the normal one.

Materials and Methods

The experiments were performed at the Marine Biological Laboratory in Woods Hole, Massachusetts, on single axons obtained from the squid, *Loligo pealei.*

The methods of axon preparation, mounting and the voltage-clamp set-up and methodology have been described previously (Adelman, Palti & Senft, 1973). Membrane currents were measured, in the voltage clamp, from axons externally perfused with artificial seawater solutions of various sodium and potassium concentrations. Tris-Cl was added to the solutions to maintain osmolarity and ionic strength approximately equal to those of the normal ASW (*see* Adelman & Palti, 1969*a*). Table 1 lists the composition of the various external solutions.

In each test solution the measurements began after membrane potential reached its new steady-state value (within 3–5 min). In between each pair of test solutions measurements were always taken in 390 mM Na ASW to monitor the condition of the axon.

Series resistance was measured in this preparation and set-up to be about $1\,\Omega\,cm^2$ (*see* Adelman *et al.*, 1973). The specific resistance of the ASW used was measured to be 24.3 Ω cm while that of the lowest conducting solution used (150 mM Na^+, 10 mM K^+ ASW) was 34.7 Ω cm. On the basis of these values and the current densities measured, the voltage shift due to the IR_s drop was calculated. Using the sodium $I-V$ curves the maximal error in I_{Na} determination was estimated to be less than 3 %.

The voltage-clamp command pulses were generated by a computer (general automation SPC-12) through a D/A convertor. Pulse amplitudes were accurate to 0.2 mV, and pulse duration to 10 μsec. Single or pairs of pulses (conditioning and test) were used. Pulse interval was 2–3 sec. In between pulses the axons were held at a potential (E_H) equal to their resting potential in normal ASW. During each experiment the membrane potential was first clamped to −105 mV for 45 msec, by a conditioning hyperpolarizing pulse. Then membrane potential was stepped to 0 mV for 5 msec.

The membrane currents were sampled by means of an 8-bit A/D convertor under program control. Sampling rates varied according to the rate of current changes. Maximum sampling rate was 200 kc. The sampled values were stored on digital magnetic tape for further analysis by means of an IBM 370/168 computer. The major end products of this analysis were the values of the peak sodium currents obtained upon membrane depolarization. These were corrected for noise, base-line shifts, leakage and potassium currents.

Table 1. Composition of the ASW solutions given in mM[a]

Solution No.	[NaCl]	[KCl]	[Tris-Cl]	[$CaCl_2$]	[$MgCl_2$]
1	430	10	–	10	50
2	390	10	40	10	50
3	250	10	180	10	50
4	150	10	280	10	50
5	390	25	25	10	50
6	250	25	165	10	50
7	150	25	265	10	50
8	390	50	–	10	50
9	250	50	140	10	50
10	150	50	240	10	50

[a] pH of all solutions was set to 7.4.

The measured inward sodium currents are actually a passage of sodium ions through the axon membrane from the outer surface to the inner surface. The current can be taken as a measure for the SIS reaction rate under the following assumptions:

1) The SIS reaction is the rate-limiting step in the transfer process.

2) Under the above experimental conditions, at the time sodium current reaches its peak, the sodium inactivation process (Hodgkin & Huxley, 1952) can be neglected ($h \simeq 1$).

3) There is no sodium accumulation in the membrane during sodium current flow.

Under these assumptions and since internal sodium concentration can be taken as homogeneous, the rate of the SIS-reaction, v, is given by:

$$v = d([Na^+]_{in})/dt = (A/F \cdot V) I_{Na} \equiv K \cdot I_{Na}$$
$$K = (F \cdot d/4)^{-1} \text{ (mol/coul cm)} \quad (1)$$

where

$[Na^+]_{in}$ = internal sodium concentration (mmol/cm^3)
I_{Na} = peak inward sodium current density (mA/cm^2)
F = Faraday constant (coul/mol)
A = surface area of the axon segment (cm^2)
V = volume of the axon segment (cm^3)
d = axon diameter (cm)
v = SIS reaction rate (mol/liter sec).

Results

I. Experimental

The peak sodium currents were measured in the given solutions from five axons. The currents measured from the axons under different conditions were normalized by referring the peak current to that measured in 150 mM $[Na^+]$, 10 mM $[K^+]$ ASW. The average values thus obtained are given in Table 2. It should be noted that by means of Eq. (1), one can translate these current density values to the SIS-reaction rate values, v, (mol/liter · sec). Moreover, in our specific case, since the reference axon diameter is $(4.5 \pm 0.1) \times 10^{-2}$ cm, the factor K in Eq. (1) equals 0.94 (mmol/coul cm). Therefore, the experimental results given in Table 2 in mA/cm^2 can be read directly to a good approximation, in moles/liter sec.

The experimental error in each current measurement was calculated taking into consideration the errors due to the limited accuracy of the 8-bit A/D convertor and the total current "noise" (± 0.05 mA/cm^2). The calculated error values corresponding to the average current measurements of Table 2 are given in Table 3. The relatively large error of the average sodium current value obtained in 430 mM Na^+ ASW is due to the fact that these measurements were performed on two, rather than five axons.

Let us assume that sodium concentration near the active sites is linearly related to sodium concentration in the bulk solution. Under this assump-

Table 2. Average values of measured inward sodium current density given in mA/cm^2

$[Na^+]$ (mM)	$[K^+]$ (mM)		
	10	25	50
430	3.20		
390	2.19	1.67	1.21
250	0.95	0.81	0.55
150	0.49	0.30	0.25

Table 3. Estimated error of the average values of sodium current densities given in Table 2 (mA/cm^2)

$[Na^+]$ (mM)	$[K^+]$ (mM)		
	10	25	50
430	1.33		
390	0.70	0.51	0.55
250	0.35	0.29	0.28
150	0.10	0.18	0.12

tion we can interpret Figs. 1–3 as illustrating the dependence of the SIS reaction rate on the concentration of the reactants, i.e. ions in the external solution.

Fig. 1 illustrates the dependence of the average peak inward sodium current on external sodium concentration at various external potassium concentrations. It is seen that external potassium inhibits inward sodium current flow.

The zero current value was put at the point where $[Na^+]_o = [Na^+]_i$. This point was calculated on the basis of the experimentally determined E_{Na} value in normal ASW.

The curves of Fig. 2 in which average $1/I_{Na}$ is plotted as a function of $1/[Na_o^+]$ are the equivalent of the Lineweaver-Burk curves. Since the curves are concave, they suggest a positive cooperativity (Appendix I, Part 2) in the sodium transfer process.

If we assume the inward sodium current saturates at some external sodium concentration value, the curves would reach the ordinate above the origin. Thus the extrapolation of the curves towards the ordinate increases their degree of nonlinearity. Note, however, that experimentally, one cannot extend the curves further towards higher sodium concentrations because of osmotic restrictions.

Fig. 3 illustrates the dependence of average inward sodium current on external potassium concentration at various external sodium concen-

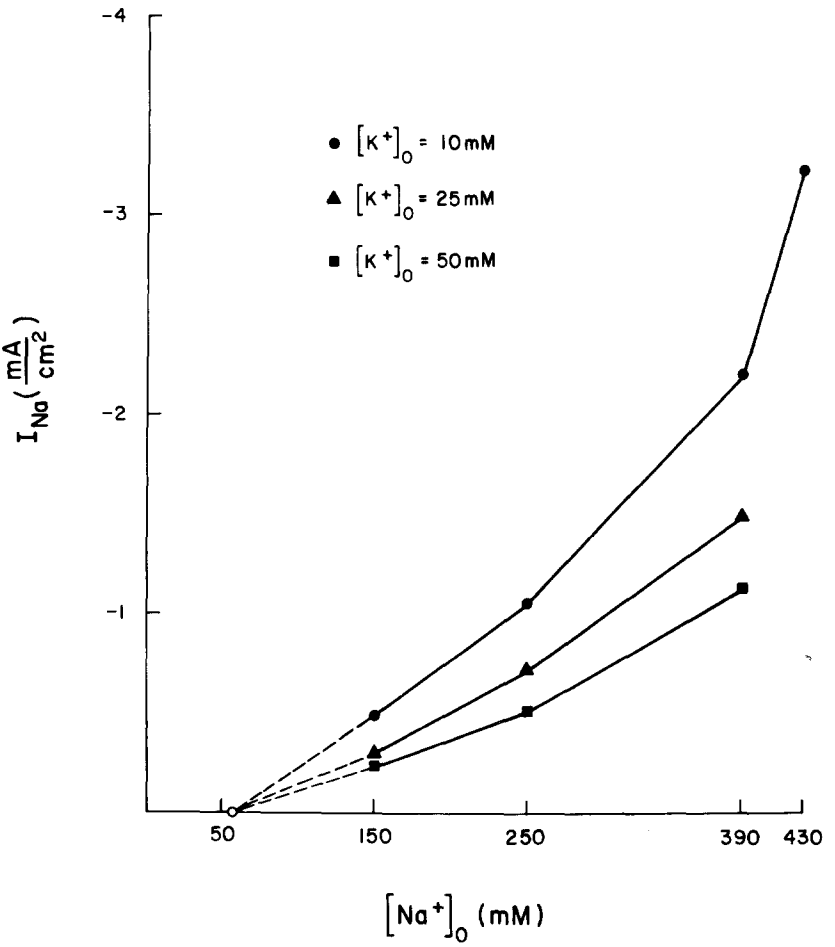

Fig. 1. Inward sodium current as a function of external sodium concentration at various external potassium concentrations. Open circle on abscissa represents the computed internal sodium concentration

trations. The sodium current values corresponding to external potassium concentrations of 3 and 5 mM were taken from Adelman and Palti (1969*b*). These additional points fall within the pattern of the curves obtained in this work.

II. Analytical

In order to determine whether the process which determines sodium current can be described by means of kinetics of saturation reactions, the experimental results were tested against a series of possible saturation reaction mechanisms. Fig. 4 summarizes some of the relevant reaction

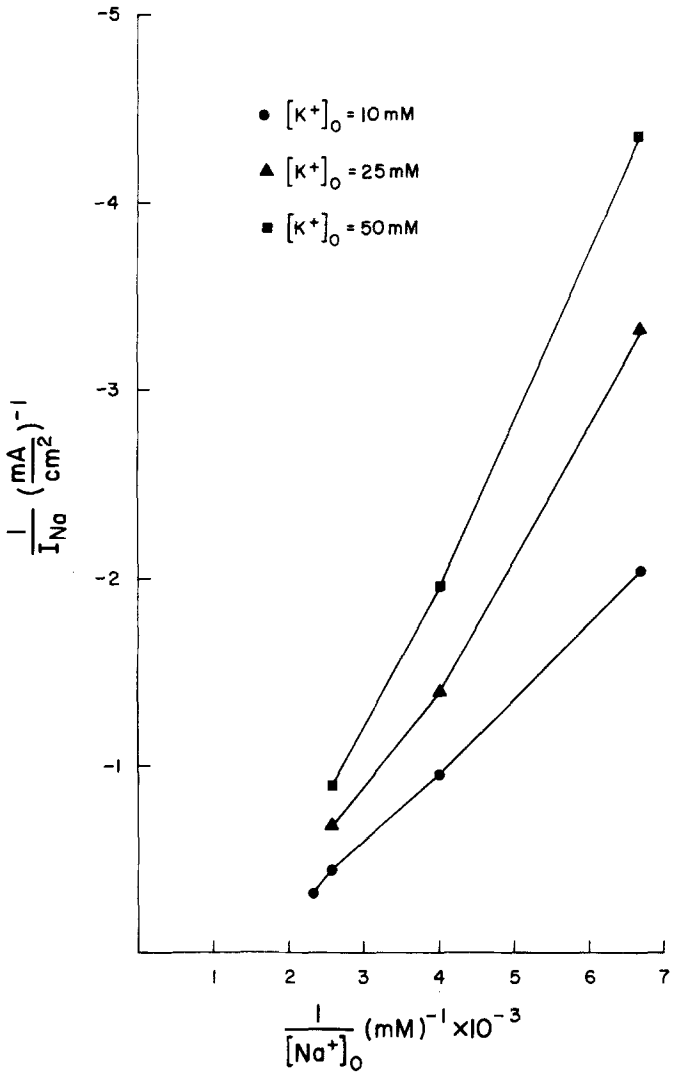

Fig. 2. The reciprocal of inward sodium current as a function of the reciprocal of external sodium concentration, at various external potassium concentrations

mechanisms studied. The equations which describe the rate of these reactions were derived by the King and Altman method (King & Altman, 1956). An example of such a derivation is given in Appendix II. These derivations are based on the following:

1) *The ion-site "complex" decomposition* is assumed to be the slowest process of the SIS-reaction. The binding of the ion to the specific site is assumed to be a fast and reversible reaction and therefore at equilibrium.

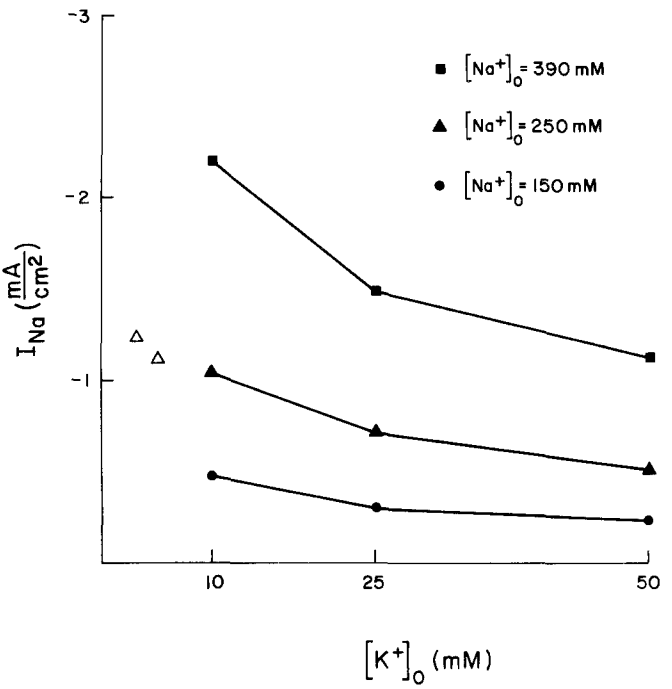

Fig. 3. Inward sodium current as a function of external potassium concentration at various external sodium concentrations

2) *Steady-state approximation.* The rate of change of the intermediates' concentration is assumed to be zero. This assumption is justified at the time of measurement, i.e. when sodium current reaches peak. At this time (*see* Eq. 1) the site occupancy reaches a steady state as sodium current activation process reaches a steady state ($m \to m_\infty$, Hodgkin & Huxley, 1952).

3) *First order kinetics* are assumed for all processes involved in the SIS reaction.

The fit of the experimental data to the various possible reaction mechanisms (*see* examples in Fig. 4) was determined by testing the data against the solutions of the appropriate rate equations by means of the minimization method of Powell (1965).

This method is designed to find the minimal sum of squares of non-linear functions. In our case the search is for the minimum of the χ^2 function. The χ^2 is defined by the following sum:

$$\chi^2 = \sum_i \frac{(V_i - I_i)^2}{(\Delta I_i)^2} \tag{2}$$

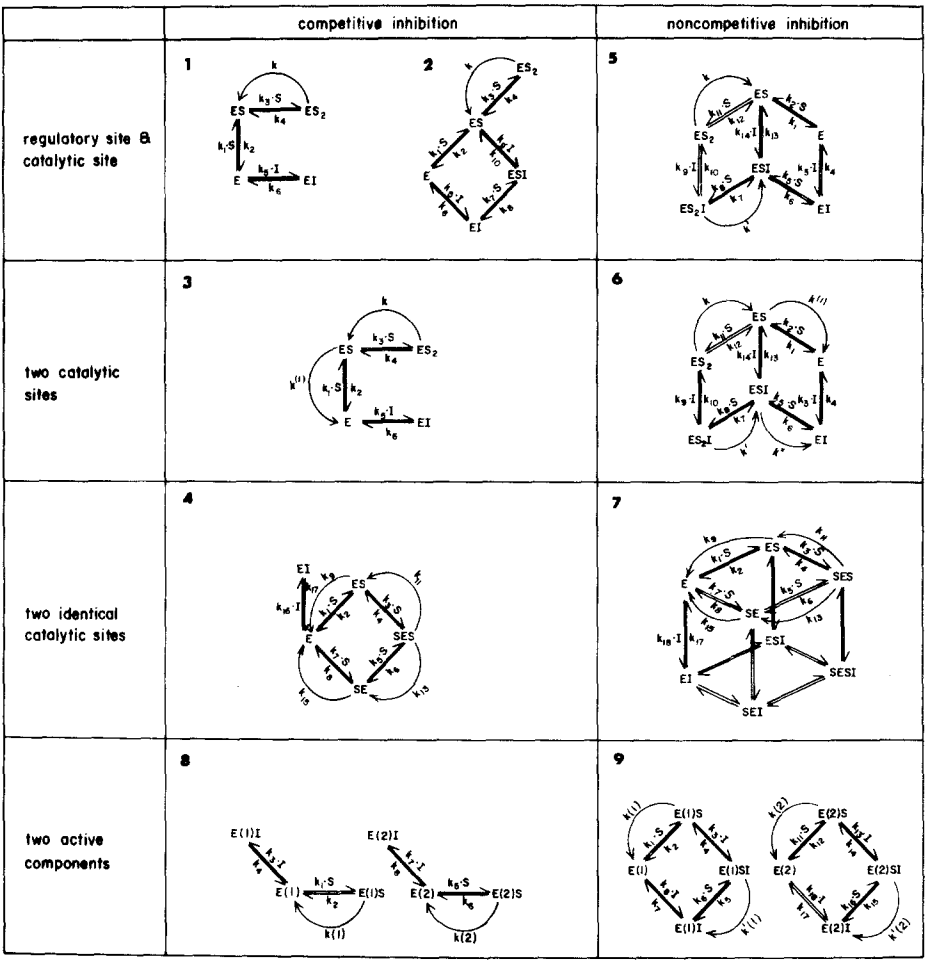

Fig. 4. Schematic representation of the analyzed reaction mechanisms of the SIS-reaction. E = active subunit of the sodium channel; S = substrate, in our case sodium ions in the external solution Na_0^+; I = membrane sodium ion conductance inhibitor, in our case, the potassium ions in the external solution K_0^+. The curved arrows represent the reaction path of the site–ion "complex" decomposition. The various intermediate complexes are represented by combinations of the symbols for each substance. The subscripts of ES and ESI denote the number of substrate molecules bound to the site. The numbers in brackets, such as $E(1)$, $E(2)$, serve to distinguish between different types of active sites catalyzing the same reaction. In schemes 4 and 7, where two identical sites are involved, ES and SE define different substrate site complexes. $k_{i=1,2\ldots n}$ = rate constants. k = rate constant of the decomposition of ion site complex. $k(1)$, $k(2)$ = rate constants of the decomposition of ion-site complex, for the two independent active sites, respectively. $k'(1)$, $k'(2)$ are the same as $k(1)$, $k(2)$, but in the presence of noncompetitive inhibition. For other definitions *see* Appendix I

where

V_i = the reaction rate (mmol/liter sec) calculated for different reaction models

Table 4. Summary of the results obtained by fitting the experimental data to the rate

Scheme No.	Mechanism			Degrees of Freedom
1	Michaelis-Menten 1st order		noncompetitive inhibition	7
2	1st order reversible reaction		noncompetitive inhibition	6
3	2 active components		competitive inhibition	4
4	2 active components		noncompetitive inhibition	4
5	cooperative n sites[b]		noncompetitive inhibition	6
6	cooperative reaction 2 sites	reg. site & cat. site	competitive inhibition in reg. reaction	6
7	cooperative reaction 2 sites	reg. site & cat. site	competitive inhibition in cat. reaction	6
8	cooperative reaction 2 sites	2 cat. sites	in 1st cat. reac.	5
9	cooperative reaction 2 sites	2 ident. cat. sites	in 1st cat. reac.	5
10	cooperative reaction 2 sites	reg. site & cat. site	noncompetitive inhibition	5
11	cooperative reaction 2 sites	2 cat. sites	noncompetitive inhibition	5
12	cooperative reaction 2 sites	2 ident. cat. sites	noncompetitive inhibition	5

[a] Reaction rates are given in mmoles/liter sec; dissociation constants are given in mM.
[b] Hill equation.

I_i = experimental value of the reaction rate, as measured by means of peak sodium currents

ΔI_i = the error in the average sodium currents estimation. This error was calculated on the basis of the experimental errors.

The end product of the minimization procedure, carried out by means of a digital computer, is:

1) An estimate of the fit of the different reaction mechanisms to the experimental data.

equations calculated for the reaction mechanisms given in Fig. 4[a]

χ^2	K_i	$K_s 10^{-3}$	$K_{2s} 10^{-3}$	k'/k	$k \cdot E_t/k_R \cdot E_t$	$k^{(1)} \cdot E_t$
7.00	Very far from physiol. range					
1.64	12.0± 7.1	0.35±0.10			7.2±1.8/33.5±17.8	
6.50	Very far from physiol. range					
6.60	Very far from physiol. range					
0.67	32.8±16.5	$\bar{n}$=1.64±0.15			51.5±42.2	
0.64	19.0± 6.4	0.55±0.30	0.66±0.10		14.0±11.4	
0.60	25.0± 7.5	0.85±0.35	0.59±0.14		16.8±12.0	
0.49	24.8± 7.5	1.28±0.68	0.70±0.30		22.1± 5.1	1.54±3.10
0.42	11.4± 6.1	1.38±1.10	0.50±0.47		16.4±14.4	2.80±4.00
0.60	15.1± 2.7	0.90±0.30	0.80±0.30	0.14±0.10	30.2±25.9	
0.44	23.7±11.0	1.92±0.70	1.17±1.55		53.8±57.5	2.90±4.30
0.40	22.7± 5.6	4.32±0.41	0.45±0.50		23.6±22.7	2.50±3.90

2) A set of parameters which give best fit to each model. These parameters are, in our case, the dissociation constants and maximal reaction rates.

The various parameters thus derived, for the different reaction mechanisms of Fig. 4, are given in Table 4.

The definition of the parameters in Table 4 is based on the classical enzyme kinetics since the SIS reaction is analogous to an enzymatic process. Within this framework sodium and potassium ions, in the external solution, are the substrate (Na_o^+) and inhibitor (K_o^+) of the SIS-reaction, while sodium ions on the inner side of the membrane (Na_i^+) are the product of the reaction. Some of the studied models involve more complex reactions.

These include cases where sodium may bind with a single or few specific sites which may interact allosterically (cooperativity).

Within this framework the parameters of Table 4 are defined as follows:

K_s = the dissociation constant of sodium ion from the sodium binding site at the external surface of the membrane

K_{2s} = same as K_s but for an additional allosteric sodium binding site

k = the rate constant of sodium-site "complex" decomposition into internal sodium

k_R = same as for k but for the reverse reaction path

k' = same as for k, but in the presence of noncompetitive inhibition (Appendix I, Part 7) by potassium

$k^{(1)}$ = same as for k, but for a regulatory site which has, in addition, catalytic activity (Fig. 4, Schemes 6 and 7)

K'' = same as for $K^{(1)}$ but in the presence of noncompetitive inhibition (Appendix I, Part 7) by potassium

E_t = the average density of active subunit of the sodium channel in the membrane segment studied.

We evaluated the fit of the experimental results to the various mechanisms studied on the basis of the following three criteria which can be determined from Table 4:

1) The χ^2 value. Using tables of χ^2 distribution, the fit of each function to the experimental results can be determined.

2) The values of the dissociation constants should be in the physiological concentration's range if the system works close to maximal efficiency.

3) The relations between the calculated rate constants and dissociation constants in each particular mechanism. For example, in a positive cooperative mechanism (*see* Appendix I, Part 3, K system) $K_{2s} < K_s$, in the case of positive cooperativity between two catalytic sites $k^{(1)} < k$ (v system), in a noncompetitive mechanism $k < k'$, and in a reversible reaction, except under unusual conditions, $k_R < k$.

However, note that the above interpretation of the parameters of the SIS reaction as rate and dissociation constants is correct only when the ion concentration is the same in the external bulk solution and near the sites.

In the Table we see that the first-order Michaelis-Menten reaction (No. 1) without a reverse path has a very high χ^2 while K_i, K_s and $K \cdot E_t$ are very far from the physiological range. In the first-order reversible Michaelis-Menten reaction (No. 2) the rate constant for the reverse reaction is four times as large as that for the forward reaction. Thus on

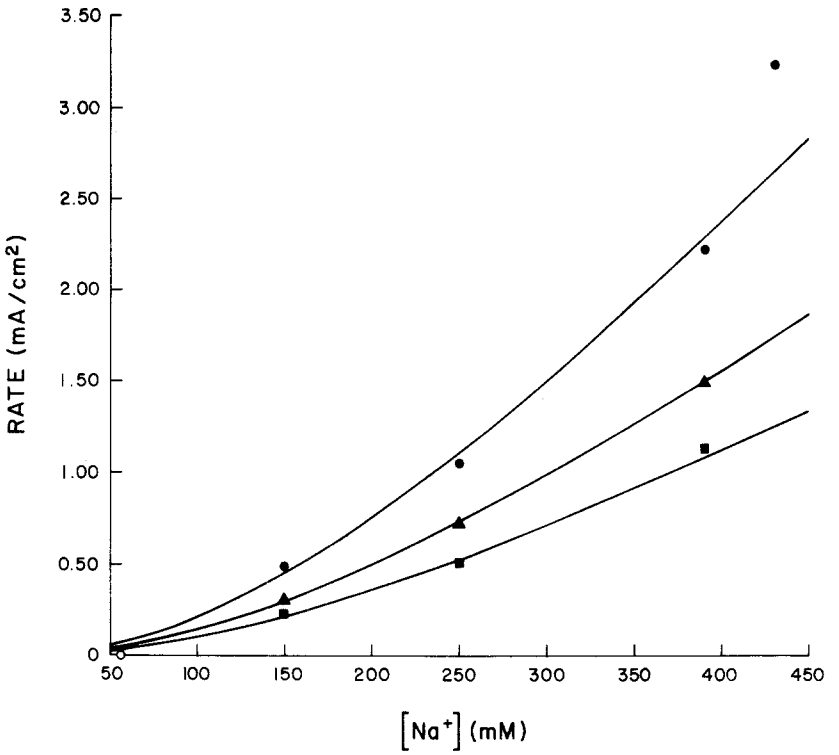

Fig. 5. Reaction rates calculated (Eq. 2) for the reaction illustrated in Fig. 4, Scheme 5, as a function of external sodium concentration. The upper curve is for $[K^+]_o = 10$ mM, the middle curve for $[K^+]_o = 25$ mM and the lower curve for $[K^+]_o = 50$ mM. The symbols give the experimental values of peak sodium current density ● $[K^+]_o = 10$ mM; ▲ $[K^+]_o = 25$ mM; ■ $[K^+]_o = 50$ mM. Open circle on abscissa represents the computed internal sodium concentration

the basis of the above criteria, one can rule out the possibility that the SIS-reaction is a first-order Michaelis-Menten reaction.

Moreover, two independent Michaelis-Menten type reactions (Nos. 3 & 4), i.e. two different types of sites each having a different affinity etc. to sodium, also give very high χ^2 values and unacceptable constants.

In contrast to the above, when the fit of the data is tested against cooperative reaction as represented by the Hill equation (Appendix I, Part 8), the χ^2 value is reasonable and K_i is in the range of potassium concentration in the external solution. In this particular case the other parameters in the equation are invalid. However, the Hill constant $\bar{n}$, (Appendix I, Part 8) which gives best fit to the data, was calculated to be about 2 ($\bar{n}$ gives the minimal number of allosteric sites).

In view of the above, we further tested the experimental data only against positive cooperative reactions involving two active sites. It is seen in the Table that for all the reactions of this type the χ^2 values give probability level of 99 % for the conditions and parameters (degrees of freedom) in question (*see* χ^2 Tables). Moreover, the dissociation constants fall within the physiological range (10 mM for K_i and 0.430 M for K_s). Note also that due to the relatively small number of sodium concentrations studied, the standard deviation values of the parameters are relatively large.

In the Table we see that the two noncompetitive inhibition reactions involving two catalytic sites (Nos. 11 & 12) give the worst fit to the experimental data. In both cases the K_s and K_{2s} are relatively high and have very large standard deviations.

The remaining five types of reactions are in good fit with the experimental data, as judged by the given criteria. Overall, the best fit perhaps is with No. 7 or No. 10 (Fig. 4, Schemes 1, 2, 5), each involving a regulatory and catalytic site. However, the inhibiting mechanism of the one is competitive while that of the other is noncompetitive.

Fig. 5 illustrates the fit of the exprimental values with the calculated reaction rate dependence on external Na^+ and K^+ concentrations for the reaction given in Scheme No. 5 in Fig. 4. The computation is based on the following equation:

$$v=\frac{kE_t(1+k'\cdot[I]/kK_i)}{(K_sK_{2s}/[S]^2+K_{2s}/[S]+1)(1+[I]/K_i)}. \tag{3}$$

The full derivation of the expression is given in Appendix II. It is seen that the measured peak sodium currents fit well the calculated values of reaction rates.[4]

Discussion

The described dependence of inward sodium current on external sodium and potassium concentrations demonstrates that the membrane sodium transfer process cannot be regarded as a two-state process with first-order kinetics. Moreover, the independence principle is clearly violated. Thus, for the given experimental conditions, one cannot depend on the Hodgkin-Huxley axon model.

An attempt was made in this work to interpret the results in terms of a specific ion-site reaction occurring at a limited number of membrane "channels".

4 It should be noted that the point of zero sodium current was not considered in the curve-fitting processes.

Within this framework, first-order Michaelis-Menten type reaction mechanisms, including those based on two types of sites differing in both affinity for sodium and dissociation rates, had to be rejected on the basis of experimental evidence. In contrast, the experimental data was found to fit well the kinetic equations of homotropic positive cooperative reactions involving at least two allosteric sites.[5] External potassium was found to act by means of a reversible inhibition – either competitive or non-competitive. Simple uncompetitive inhibition was rejected.

As the membrane channels are relatively far apart (Keynes, Ritchie & Rojas, 1971), the two (or more) allosteric sites must be part of the same channel. One of these sites may be regulatory while the other a catalytic site. However, both may be catalytic, i.e. directly involved with the transfer process. Thus one may regard the sodium channel as consisting of a macromolecule, or a few closely interacting macromolecules, having at least two active sites (Fig. 6).

Sodium may bind to and be transferred across the membrane by means of either one of these sites. When it binds to or interacts with one of the sites it may facilitate both the rate of binding and dissociation of another sodium from the second allosteric site, i.e., it facilitates the ion transfer across the membrane (cooperativity)[6]. Were the mechanism of inhibition competitive, potassium ion may bind to either one of the sites and block the sodium transfer at this site (Fig. 6, Schemes 3 and 4).

The experimental data is consistent with the idea that one of the sites is regulatory (*r* in Fig. 6) while the other is catalytic (*c* in Fig. 6). Therefore, one can visualize that when sodium binds to the regulatory site (which in itself does not transfer ions) the sodium transfer is enhanced (Fig. 6, Schemes 5 and 6), while when potassium is bound to it, the process is inhibited (Fig. 6, Schemes 7 and 9). This model is in agreement with Hille's (1975) recent channel model consisting of a "binding site" as well as a regulatory element.

Fig. 5 gives a schematic description of a number of additional competitive and noncompetitive mechanisms of the types studies (*see* Fig. 4). The given models of the sodium channel are based on sodium currents measured at a single membrane potential. Therefore, they have no direct bearing on the voltage dependency of the sodium conductance mechanism

5 It should be noted that Squires (1965) studied the effect of sodium concentration on Na^+-K^+ATPase (from rat brain) and reported that the activity fits a cooperative mechanism involving at least two allosteric sites.

6 The relaxation times of macromolecule conformation changes are compatible with the duration of ion dwell time in the membrane.

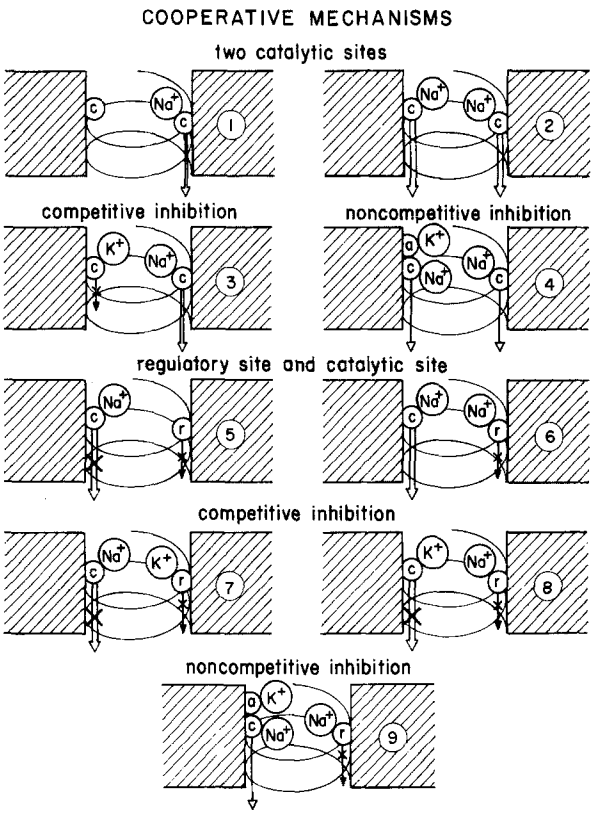

Fig. 6. Schematic representation of the SIS-reaction mechanism in sodium channel. c = catalytic site; r = regulatory site; a = additional allosteric site. All sites are part of a hypothetical macromolecule (spiral). The arrow thickness represents the SIS reaction rate or rate of sodium transfer *(see text)*

(parameters m & h). Therefore on the basis of the given results one cannot determine whether the sites in question which determine the potassium conductance g_K are part of the sodium activation "m" or inactivation "h" system. However, the analysis of Adelman and Palti (1969*a*, *b*) indicates that the potassium effects on sodium currents can be best described by an effect on the sodium inactivation. Also, Fishman *et al.* (1973) have analyzed the potassium inhibitory effect in similar terms. Therefore, it is probable that the mechanisms described in this work may be a part of the sodium inactivation system.

On the basis of this work, it can be concluded that the nerve membrane sodium conductance mechanism can be described in terms of a complex ion-channel interaction. The process involves interaction or binding with a number of active sites and probably involves a number of stages (Palti,

Stampfli, Ganot & Ehrenstein, 1975). These findings, together with the recent evidence for large dipole moment and conformational changes associated with the opening and closing of the channels (Levitan & Palti, 1975), imply that the sodium channel is a rather large structure. Thus, it seems reasonable to conclude that most probably it consists of at least one large polar macromolecule having a few active subunits which show specific ionic interaction.

Appendix I

Definitions of Terms used by Analogy to Enzyme Kinetics
(Mahler & Cordes, 1966; Boyer, Landy & Myrback, 1959)

1. *Active Site (catalytic site).* The existence of certain relatively small areas on the active molecules (in the sodium channel) is believed to account for their properties and conveniently referred to as active centers or active sites.

2. *Cooperativity.* Modulation of the molecule activity through the binding of small molecules at specific sites, which are distinct from the active site, termed allosteric sites. Positive cooperativity indicates enhancement of catalytic activity. An activator is a molecule, the effect of which is positive cooperativity.

3. *Allosteric Effect.* A term used generally to describe the interaction of any small molecules, including the substrate, at binding sites other than the catalytically active site of an enzyme. These molecules are called allosteric effectors. The effect of the allosteric binding on the enzyme activity is called "allosteric effect". Allosteric effectors may either influence the affinity of the active site for the substrate (K system) or the rate of decomposition of substrate-enzyme-"complex" to products (V system) or both.

4. *Regulatory Site.* An allosteric site on the active molecule in sodium channel where effectors bind and thereby modulate its activity.

5. *Homotropic Effect.* Cooperativity where the allosteric effector is a substrate molecule.

6. *Competitive Inhibition.* Inhibition due to the binding of the inhibitor to the substrate binding site. Since binding is reversible, the inhibition may be overcome by increasing substrate concentration.

7. *Noncompetitive Inhibition.* Inhibition of the rate of decomposition of substrate site "complex" where the substrate and inhibitor can bind simultaneously with different sites on the enzyme.

8. *Uncompetitive Inhibition.* Inhibition of the dissociation of substrate-site "complex" into products. As the inhibitor binds to the substrate site "complex," the inhibition cannot be abolished by increasing the substrate concentration.

9. *Hill Equation.* Derived to describe the kinetics of hemoglobin binding with oxygen, where binding of each oxygen molecule increases the affinity of the protein for the next. By analogy, homotropic cooperation phenomena in enzyme kinetics have frequently been expressed in terms of an equivalent Hill equation:

$$\log \frac{v}{V-v} = n \log s - \log K \quad \text{or} \quad v = \frac{V \cdot S^n}{K + S^n}$$

where V = maximal reaction rate, S = substrate concentration, n = minimal number of allosteric sites, and K = a constant.

This equation has the form of a general binding equation except that the concentration of all intermediates, such as ES_1, ES_2 and ES_{n-1}, are assumed to be negligible. This, in effect, means that infinite cooperativity has been assumed in the derivation of this equation, i.e. the binding of first molecule of ligand is immediately followed by the binding of all subsequent molecules of ligand. In such systems $n_{\text{Hill}}(\bar{n})$ should equal the number of allosteric sites. However, in practice this is a theoretical limit which is never completely satisfied.

Thus as a first approximation, Hill coefficients, derived from velocity studies, can be used as an indication of the minimum number of sites.

A Hill coefficient greater than one indicates positive cooperativity, less than one-negative cooperativity, and a coefficient of one-noninteracting sites.

Appendix II

Derivation of the Expression for the SIS-Reaction Rate, v, of the Cooperative Mechanism Illustrated in Scheme 5 of Fig. 4

In the given reaction the substrate reacts with two allosteric active sites, one of which has a regulatory function while the other is a catalytic site. The reaction is inhibited in a noncompetitive mechanism. Sodium and potassium ions in the external solution are the substrate and inhibitor of the SIS-reaction, respectively.

The mechanism of noncompetitive inhibition requires that $k' < k$. Since this reaction involves a regulatory site, zero should be substituted for the dissociation rate constants $k^{(1)}$ and k'' of both the site-substrate "complex" (ES) and site-substrate inhibitor "complex" (ESI).

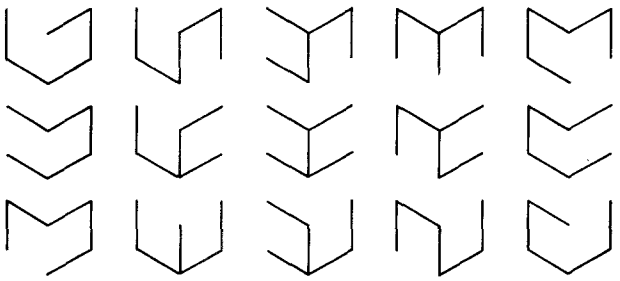

Fig. 7. Five-lined pattern paths of the reaction mechanism given in Fig. 4, Scheme 5. According to the King and Altman method

On the basis of the assumptions given in Materials and Methods, the SIS-reaction rate or rate of appearance of products is given by:

$$v = k \cdot [ES_2] + k'[ES_2 I] - k_R[ES] \cdot [P] - k'_R[ESI] \cdot [P] \qquad \text{(A.1)}$$

where E = active subunit of the sodium channel, S = substrate, I = inhibitor, and P = product.

The various intermediate "complexes" are represented simply by combination of the symbols for each substance. The subscripts of ES and ESI denote the number of substrate molecules bound to the sites.

As the computed value of the reverse reaction rate constant was negligible, the terms expressing the reverse reaction rate were not considered. Since we are dealing with a reaction in a steady-state condition (*see* assumption in the Results section) we can use the King and Altman method (King & Altman, 1956) to solve the rate equations and obtain the expression for the reaction rate v.

This method simplifies the solution by using a graphic, instead of the conventional algebraic solution using determinant based on Crammer's rules. According to the King and Altman method for this reaction where six intermediate "complexes" are involved, the total number of five-lined patterns (except for closed loops) is:

$$\frac{7!}{5!2!} - 6 = 15.$$

The various patterns are represented in Fig. 7.

The expression obtained for the intermediate complexes' concentration in the steady-state conditions ($[ES]$, $[ESI]$ etc.) are the same as obtained using Crammer's rules. The denominator in each expression which is the

coefficient determinant of the set of the rate equations, is not explicitly written but denoted as "denom". In this case the denominator is the sum of all nominators.

The expressions obtained for the concentration of each intermediate complex are:

$$\begin{aligned}\frac{[E]}{E_t}\text{(denom)} &= k_1k_4k_6k_{10}(k_{12}+k)+k_1k_4k_6(k_7+k')(k_{12}+k)+k_1k_4k_6(k_7+k')k_9\cdot I\\ &\quad +k_4k_6k_{10}(k_{12}+k)k_{14}\cdot I+k_4k_6(k_7+k')(k_{12}+k)k_{14}\cdot I\\ &\quad +k_4k_6(k_7+k')k_9k_{14}\cdot I^2+k_1k_5k_{10}(k_{12}+k)k_{13}\cdot S\\ &\quad +k_1k_5(k_7+k')(k_{12}+k)k_{13}\cdot S+k_1k_5(k_7+k')k_9k_{13}\cdot I\cdot S\\ &\quad +k_1k_4k_{10}(k_{12}+k)k_{13}+k_1k_4(k_7+k')(k_{12}+k)k_{13}\\ &\quad +k_1k_4(k_7+k')k_9k_{13}\cdot I+k_4k_6(k_7+k')k_9k_{11}\cdot S\cdot I\\ &\quad +k_1k_5k_8k_{10}(k_{12}+k)\cdot S^2+k_1k_4k_8k_{10}(k_{12}+k)\cdot S.\end{aligned} \tag{A.2}$$

$$\begin{aligned}\frac{[ES]}{E_t}\text{(denom)} &= k_2k_4k_6k_{10}(k_{12}+k)\cdot S+k_2k_4k_6(k_7+k')(k_{12}+k)\cdot S\\ &\quad +k_2k_4k_6(k_7+k')k_9\cdot S\cdot I+k_3k_5k_{10}(k_{12}+k)k_{13}\cdot I\cdot S\\ &\quad +k_3k_5(k_7+k')(k_{12}+k)k_{13}\cdot I\cdot S+k_3k_5(k_7+k')k_9k_{13}\cdot S\cdot I^2\\ &\quad +k_2k_5k_{10}(k_{12}+k)k_{13}\cdot S^2+k_2k_5(k_7+k')(k_{12}+k)k_{13}\cdot S^2\\ &\quad +k_2k_5(k_7+k')k_9k_{13}\cdot S^2+k_2k_4k_{10}(k_{12}+k)k_{13}\cdot S\\ &\quad +k_2k_4(k_7+k')(k_{12}+k)k_{13}\cdot S+k_2k_4(k_7+k')k_9k_{13}\cdot S\cdot I\\ &\quad +k_3k_5k_8k_{10}(k_{12}+k)\cdot S^2\cdot I+k_2k_5k_8k_{10}(k_{12}+k)\cdot S^3\\ &\quad +k_2k_4k_8k_{10}(k_{12}+k)\cdot S^2.\end{aligned} \tag{A.3}$$

$$\begin{aligned}\frac{[ES_2]}{E_t}\text{(denom)} &= k_2k_4k_{10}k_6k_{11}\cdot S^2+k_2k_4k_6(k_7+k')k_{11}\cdot S^2+k_1k_3k_5k_8k_{10}\cdot S^2\cdot I\\ &\quad +k_3k_5k_{10}k_{11}k_{13}\cdot S^2\cdot I+k_3k_5(k_7+k')k_{11}k_{13}\cdot S^2\cdot I\\ &\quad +k_3k_5k_8k_{10}k_{14}\cdot I^2\cdot S+k_2k_5k_{10}k_{11}k_{13}\cdot S^3\\ &\quad +k_2k_5(k_7+k')k_{11}k_{13}\cdot S^3+k_2k_5k_8k_{10}k_{14}\cdot S^3\cdot I+k_2k_4k_{10}k_{11}k_{13}\cdot S^2\\ &\quad +k_2k_4(k_7+k')k_{11}k_{13}\cdot S^2+k_2k_4k_8k_{10}k_{14}\cdot S^2+k_3k_5k_8k_{10}k_{11}\cdot S^3\cdot I\\ &\quad +k_2k_5k_8k_{10}k_{11}\cdot S^4+k_2k_4k_8k_{10}k_{11}\cdot S^3.\end{aligned} \tag{A.4}$$

$$\begin{aligned}\frac{[EI]}{E_t}\text{(denom)} &= k_1k_3k_6k_{10}(k_{12}+k)\cdot I+k_1k_3k_6(k_7+k')(k_{12}+k)\cdot I\\ &\quad +k_1k_3k_6(k_7+k')k_9\cdot I^2+k_3k_6k_{10}(k_{12}+k)k_{14}\cdot I^2\\ &\quad +k_3k_6(k_7+k')(k_{12}+k)k_{14}\cdot I^2+k_3k_6(k_7+k')k_9k_{14}\cdot I^3\\ &\quad +k_2k_6k_{10}(k_{12}+k)k_{14}\cdot I\cdot S+k_2k_6(k_7+k')(k_{12}+k)k_{14}\cdot S\cdot I\end{aligned} \tag{A.5}$$

$$
\begin{aligned}
&+k_2k_6(k_7+k')k_9k_{14}\cdot S\cdot I+k_1k_3k_{10}(k_{12}+k)k_{13}\cdot I\\
&+k_1k_3(k_7+k')(k_{12}+k)k_{13}\cdot I+k_1k_3(k_7+k')k_9k_{13}\cdot I^2\\
&+k_3k_6(k_7+k')k_9k_{11}\cdot S\cdot I^2+k_2k_6(k_7+k')k_9k_{11}\cdot S^2\cdot I\\
&+k_1k_3k_8k_{10}(k_{12}+k)\cdot S\cdot I.
\end{aligned}
$$

$$
\frac{[ESI]}{E_t}(\text{denom})
$$

$$
\begin{aligned}
&=k_1k_3k_5k_{10}(k_{12}+k)\cdot I\cdot S+k_1k_3k_5(k_7+k')(k_{12}+k)\cdot S\cdot I\\
&+k_1k_3k_5(k_7+k')k_9\cdot S\cdot I^2+k_3k_5k_{10}(k_{12}+k)k_{14}\cdot S\cdot I^2\\
&+k_3k_5(k_7+k')(k_{12}+k)k_{14}\cdot S\cdot I^2+k_3k_5(k_7+k')k_9k_{14}\cdot I^3\cdot S\\
&+k_2k_5k_9k_{11}k_{13}\cdot S^3\cdot I+k_2k_5(k_7+k')(k_{12}+k)k_{14}\cdot S^3\cdot I\\
&+k_2k_5(k_7+k')k_9k_{14}\cdot S^3\cdot I^2+k_2k_4k_9(k_{12}+k)k_{13}\cdot S^2\\
&+k_2k_4(k_7+k')(k_{12}+k)k_{14}\cdot S^2\cdot I+k_2k_4(k_7+k')k_9k_{14}\cdot S^2\cdot I\\
&+k_3k_5(k_7+k')k_9k_{11}\cdot S^3\cdot I^2+k_2k_5(k_7+k')k_9k_{11}\cdot S^4\cdot I\\
&+k_2k_4(k_7+k)k_9k_{11}\cdot S^3.
\end{aligned}
\tag{A.6}
$$

$$
\frac{[ES_2I]}{E_t}(\text{denom})
$$

$$
\begin{aligned}
&=k_2k_4k_6k_9k_{11}\cdot S^2\cdot I+k_1k_3k_5k_8(k_{12}+k)\cdot S^2\cdot I+k_1k_3k_5k_8k_9\cdot I^2\cdot S^2\\
&+k_3k_5k_9k_{11}k_{13}\cdot I^2\cdot S^2+k_3k_5k_8(k_{12}+k)k_{14}\cdot I^2\cdot S^2\\
&+k_3k_5k_8k_9k_{14}\cdot I^3\cdot S^2+k_2k_5k_9k_{11}k_{13}\cdot S^3\cdot I\\
&+k_2k_5k_8(k_{12}+k)k_{14}\cdot S^3\cdot I+k_2k_5k_8k_9k_{14}\cdot S^3\cdot I^2\\
&+k_2k_4k_9k_{11}k_{13}\cdot S^2\cdot I+k_2k_4k_8(k_{12}+k)k_{14}\cdot S^2\cdot I\\
&+k_2k_4k_8k_9k_{14}\cdot S^2\cdot I^2+k_3k_5k_8k_9k_{11}\cdot S^3\cdot I^2+k_2k_5k_8k_9k_{11}\cdot S^4\cdot I\\
&+k_2k_4k_8k_9k_{11}\cdot S^3\cdot I.
\end{aligned}
\tag{A.7}
$$

In Eqs. (A.2)–(A.7) $k_{i=1,2,\ldots,n}$ rate constants; k = rate constant of substrate-site "complex" decomposition to products; k' = same as k but with non-competitive inhibition.

Assuming that as a first approximation the ion-site binding reaction is at equilibrium state (*see* Materials and Methods), we can write the following relations:

$$
k \ll k_{12}; \quad k' \ll k_6. \tag{A.8}
$$

Under the above conditions, the mechanism of noncompetitive inhibition gives the relations:

$$
\frac{k_1}{k_2}=\frac{k_6}{k_5}; \quad \frac{k_{12}}{k_{11}}=\frac{k_7}{k_8}; \quad \frac{k_4}{k_8}=\frac{k_{13}}{k_{14}}=\frac{k_{10}}{k_9}. \tag{A.9}
$$

Let us substitute the appropriate values (Eqs. A.4 and A.5) for $[ES_2]$ and $[ES]$ in the expression for v (Eq. A.1). Let us now divide the nominator

and denominator of the new expression thus derived by the nominator of the expression for $[ES_2]$ (Eq. A.5). Using the relations of Eqs. (A.9), a simple expression for v is obtained:

$$v=\frac{k\cdot E_t\left(1+\frac{k'}{k}[I]\frac{k_3}{k_4}\right)}{\left(\frac{k_{12}}{k_{11}}\cdot\frac{k_1}{k_2}\cdot\frac{1}{[S]^2}+\frac{k_{12}}{k_{11}}\cdot\frac{1}{[S]}+1\right)\left(1+[I]\frac{k_3}{k_4}\right)}. \tag{A.10}$$

Under the given conditions one can express the rate constants by measurable dissociation constants as follows:

$$\frac{k_1}{k_2}=K_s;\quad \frac{k_{12}}{k_{11}}=K_{2s};\quad \frac{k_4}{k_3}=K_i \tag{A.11}$$

where K_s = dissociation constant of substrate – regulatory site, K_{2s} = dissociation constant of substrate – catalytic site, and K_i = dissociation constant of inhibitor-site "complex".

From relationships (A.10) and (A.11) we can derive the expression for the reaction rate v:

$$v=\frac{k\cdot E_t\left(1+\frac{k'}{k}[I]/K_i\right)}{(K_s\cdot K_{2s}/[S]^2+K_{2s}/[S]+1)(1+[I]/K_i)}. \tag{A.12}$$

This expression gives the SIS-reaction rate, as a function of sodium $[S]$ and potassium $[I]$ ion concentration in the external solution.

References

Adelman, W.J., Jr., Palti, Y. 1969*a*. The influence of external inactivation of sodium currents in the giant axon of the squid *Loligo pealei*. *J. Gen. Physiol.* **53**:685

Adelman, W. J., Jr., Palti, Y. 1969*b*. The effect of external potassium and long duration voltage conditioning on the amplitude of sodium currents in the giant axon of the squid, *Loligo pealei*. *J. Gen. Physiol.* **54**:589

Adelman, W.J., Jr., Palti, Y., Senft, J. 1973. Potassium ion accumulation in a periaxonal space and its effect on the measurement of membrane potassium ion conductance. *J. Membrane Biol.* **13**:387

Boyer, P.D., Lardy, H., Myrback, K., editors. 1959. The Enzymes. Second Ed., Part I, II. Academic Press, New York

Ehrenstein, G., Lecar, H. 1972. The mechanism of signal transmission in nerve axons. *Annu. Rev. Biophys. Bioeng.* **1**:347

Fishman, S.N., Cherneikin, V.A., Volkenstein, M.V. 1973. Role of ion exchange processes in the mechanism of sodium conductance changes in excitable membranes. *Biochim. Biophys. Acta* **298**:710

Hille, B. 1968. Pharmacological modifications of the sodium channel of frog nerve. *J. Gen. Physiol.* **51**:199

Hille, B. 1972. The permeability of the sodium channel to metal cations in myelinated nerve. *J. Gen. Physiol.* **59**:637

Hille, B. 1975. A four barrier model of the sodium channel. *Biophys. J. (Abstr.)* 19th Annual Meeting

Hodgkin, A.L., Huxley, A.F. 1952. A quantitative description of membrane current and its application to conduction and excitation in nerve. *J. Physiol.* **117**:500

Hodgkin, A.L., Keynes, R.D. 1955*a*. Active transport of cations in giant axons from sepia and loligo. *J. Physiol.* **128**:28

Hodkin, A.L., Keynes, R.D. 1955*b*. The potassium permeability of a giant nerve fibre. *J. Physiol.* **128**:61

Keynes, R.D., Ritchie, J.M., Rojas, E. 1971. The binding of tetrodotoxin to nerve membrane. *J. Physiol.* **213**:235

King, E.L., Altman, C. 1956. A schematic method of deriving the rate laws for enzyme-catalyzed reactions. *J. Phys. Chem.* **60**:1375

Levitan, E., Palti, Y. 1975. Dipole moment, enthalpy and entropy changes of Hodgkin-Huxley type kinetic units. *Biophys. J.* **15**:239

Mahler, H.R., Cordes, E.H. 1966. Biological Chemistry. International Editions, New York

Palti, Y., Stampfli, R., Ganot, G., Ehrenstein, G. 1975. The effect of conditioning potential on potassium current kinetics in the frog node. *Biophys. J. (Abstr.)*, 19th Annual Meeting

Powell, M.J.D. 1965. An efficient method for finding the minimum of a function of several variables without calculating derivatives. *Computer J.* **7**:155

Squires, R.F. 1965. On the interaction of Na^+, K^+, Mg^{++} and ATP with the Na^+ plus K^+ activated ATPase from rat brain. *Biochem. Biophys. Res. Commun.* **19**:27